NANO LETTERS

pubs.acs.org/NanoLett Letter

Smart Magnetic Optical Antenna for Automatic Nanoalignment and Photon Beaming from Prepatterned Single Quantum Dot Nanospot

Luping Wang,[§] Zaiqin Man,[§] Yang Liu, Ying Yu, Chenyu Dong, Jie Bian, Yan-qing Lu,* Zhenda Lu,* and Weihua Zhang*

Cite This: *Nano Lett.* 2023, 23, 1539−1545 Read Online

ACCESS | Metrics & More | Article Recommendations | Supporting Information

ABSTRACT: We present a unidirectional dielectric optical antenna, which can be chemically synthesized and controlled by magnetic fields. By applying magnetic fields, we successfully aligned an optical antenna on a prepatterned quantum dot nanospot with accuracy better than 40 nm. It confined the fluorescence emission into a 16-degree wide beam and enhanced the signal by 11.8 times. Moreover, the position of the antenna, and consequently the beam direction, can be controlled by simply adjusting the direction of the magnetic fields. Theoretical analyses show that this magnetic alignment technique is stable and accurate, providing a new strategy for building high-performance tunable nanophotonic devices.

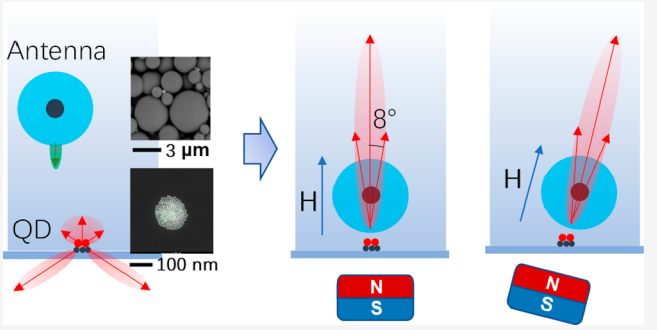

KEYWORDS: *optical antenna, smart nanomaterials, angular radiation pattern, superparamagnetic nanoparticles*

Downloaded via NANJING UNIV on May 11, 2025 at 00:04:30 (UTC).
See https://pubs.acs.org/sharingguidelines for options on how to legitimately share published articles.

Nanoemitters transmit photons in all directions since the momentum and position of photons cannot be simultaneously determined due to Heisenberg's uncertainty principle. This leads to one of fundamental challenges in nanophotonics, how to confine the radiation of a nanoemitter into a desired direction and improve its coupling efficiency in miniaturized photonic devices, such as light emission devices,[1,2] single photon sources[3,4] and bio/chem-sensors.[5,6] To address the above challenge, researchers borrowed the idea of an antenna in the radio frequency[7−9] and developed a variety of optical antennas to control the optical properties of nanoemitters.[10,11] Particularly, by placing a nanoemitter at the feed point of an optical antenna, one can direct its emission into predefined directions with a high efficiency.[4,12−16]

In practice, it is however challenging to obtain such an emitter−antenna coupling system. It not only requires expensive nanolithography processes to fabricate an optical antenna but also needs techniques to precisely align the optical antenna with a nanoemitter. So far, this nanoscale heterogeneous integration can only be achieved with the help of nanoassembly techniques[17,18] and scanning-probe-based manipulation methods.[19−23] Both methods are sophisticated and technically challenging. Moreover, most optical antennas are static, except a few attempts with MEMS technique and phase transition materials.[24−27] There is a lack of simple yet effective methods to tune the coupling between optical antenna and nanoemitter, leading to many limits on the optical antenna technique.

Interestingly, there have been many exciting developments in the field of colloidal chemistry recently, and "smart" micro/nano-particles with special optical properties have been demonstrated.[28−30] By composing different functional nanomaterials together, one can create a nanorobot which can be selectively and precisely guided to a nanotarget.[31−33] Meanwhile, it was reported that a dielectric colloidal microsphere can function as an optical antenna which can create a tight focus, generate beam-like emission, and consequently enhance the signal significantly.[34−40] Intrigued by above developments, here, we combine the idea of nanorobot with dielectric optical antenna together, and propose a new smart optical antenna (SOA). The SOA can be chemically synthesized and dynamically controlled with external magnetic fields, providing a simple but powerful method for engineering the radiation of nanoemitters.

Figure 1 shows the principle of the magnetic alignment of the SOA, which are chemically synthesized polystyrene microspheres (ranging from 0.5 to 5 μm) with superparamagnetic core (approximately 400 nm in diameter). To guide the SOA and realize high precision alignment, we assembled quantum dots (QDs) together with 10 nm superparamagnetic nanoparticles (NPs) into a magnetic QD nanospot using the nanoprinting technique developed by the same authors.[41] When magnetic

Received: December 21, 2022
Revised: January 19, 2023
Published: February 7, 2023

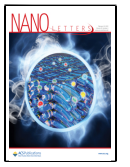

ACS Publications © 2023 American Chemical Society

https://doi.org/10.1021/acs.nanolett.2c04981
Nano Lett. 2023, 23, 1539−1545

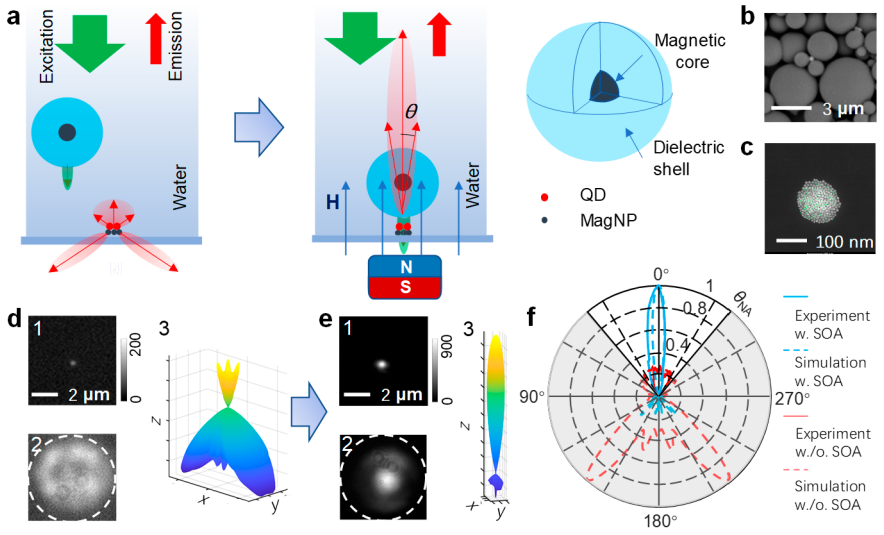

Figure 1. Magnetic alignment and photon beaming of the smart optical antenna. (a) Principle of magnetic alignment of SOA. (b and c) Electron micrograph of SOA and nanoprinted magnetic QD nanospot, respectively. (d and e) Results of QD nanospot with and without SOA, respectively. Panel 1−3 is the fluorescence image, angle radiation pattern (back focal plane image) and simulated angular radiation pattern, respectively. The dashed line labels the observation area of the objective (sin θ_{NA} = 0.6). (f) Angular radiation pattern in the $X-Z$ plane with and without SOA.

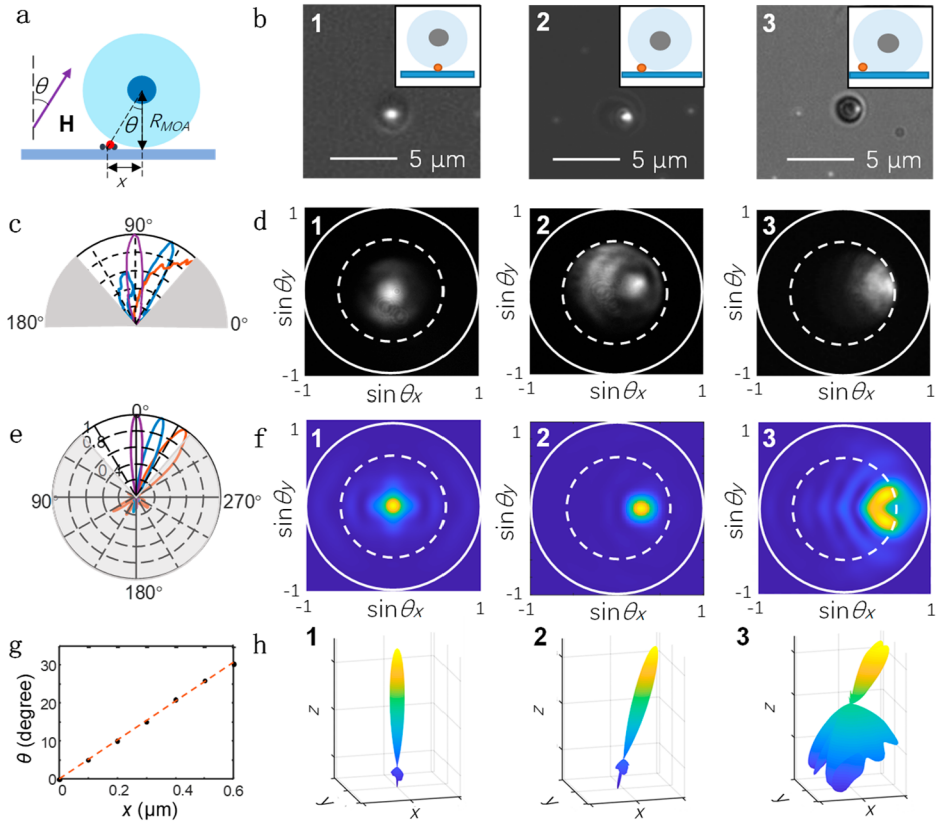

Figure 2. Position and beam direction tuning with magnetic fields. (a) Principle of the direction-dependent magnetic alignment of SOA. (b1−b3) Fluorescence images of a SOA aligned at different locations of a QD nanospot. (c) Angular radiation distributions of the fluorescence image in (b) in the $X-Z$ plane. (d1−d3) The back-focal plane images of the (b1−b3), respectively. (e) Simulated angular radiation pattern in the $X-Z$ plane for Δx = 0, 0.3, 0.6 μm. (f1−f3) The corresponding 2D radiation patterns in (e). (g) Beam direction vs Δx curve. (h1−h3) 3D view of the radiation patterns in (f1−f3). Data are normalized in (c, e, f, and h).

fields are applied, SOAs and magnetic QD nanospots will be magnetized. Then, SOAs in the solution will be captured and precisely aligned with QD nanospots along magnetic field lines via magnetic dipole−dipole interactions, as depicted in Figure 1a.

We experimentally verified this magnetic alignment technique using a 2.2 μm SOA with perpendicular magnetic fields. The

https://doi.org/10.1021/acs.nanolett.2c04981
Nano Lett. 2023, 23, 1539−1545

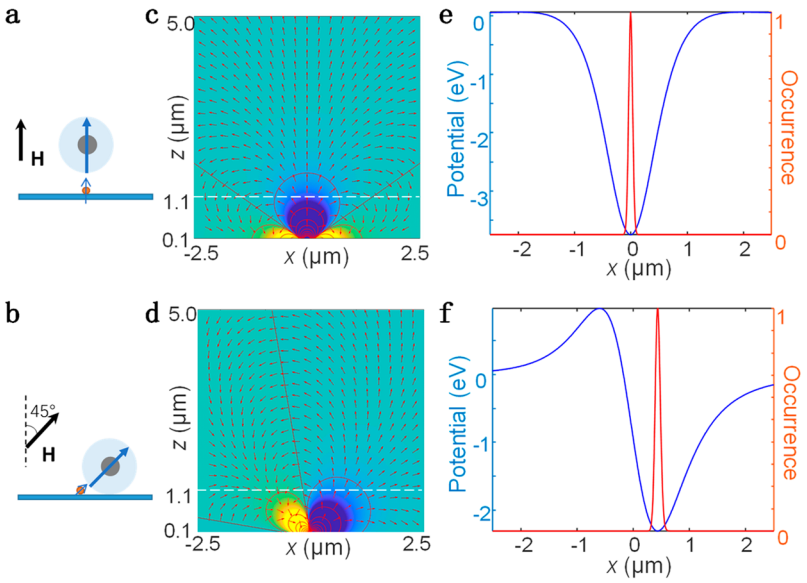

Figure 3. Magnetic interaction and alignment accuracy of SOA. (a and b) Magnetic dipole−dipole interaction between SOA and QD nanospot with magnetic fields, *H*, at 0 and 45°, respectively. (c and d) The potential map of the magnetic interactions for the case in (a and b), respectively. (e and f) Potential distribution of SOA at z = 1.1 μm, and the corresponding occurrence possibility distribute of SOA for the case in (a and b), respectively.

whole alignment process was recorded using a home-built optical system which can take images at both the sample plane and the back focal plane simultaneously (Section 1 in Supporting Information). Results show that SOAs can indeed be captured and aligned right above a QD nanospot when it swam across (Section 2 in Supporting Information).

The alignment of SOA can bring significant signal enhancement. Figure 1d,e shows a typical example, in which the fluorescence signal was enhanced by 11.8 times after the SOA was aligned. We attribute this enhancement to the high directivity of the SOA which increases the collection efficiency of the optical system. To prove this point, we recorded the radiation pattern of the same QD nanospot (i.e., the field distribution at the back focal plane). As shown in Figure 1d,e, without the SOA, photons were radiated to all directions; once the SOA was aligned on the QD nanospot, photons were confined into a beam with a half power beam width (HPBW) of 16°.

To further understand the beaming effect, simulations were performed using the finite-differential time-domain technique (FDTD). As shown by the dashed lines in Figure 1f, with a SOA, most of the light is confined into a narrow beam toward the solution side (i.e., forward direction), and the HPBW is approximately 14°, consistent with the experimental result. Only a small portion of light is coupled into the substrate side (i.e., backward direction), and the forward-to-backward ratio of the radiation reaches 8.70 dB. On the contrary, without the SOA, most of light (70.1%) is coupled to the substrate side (i.e., backward), and in the solution side, light is emitted to all angles. As a result, the coupling efficiency of the system is low, and only small fraction of the light can be collected by the objective lens (N.A. = 0.6, maximum collection angle is 36.9°). This explains the observed signal enhancement.

In antenna theory, the above unidirectional radiation behavior of the SOA can be quantitatively described by "directivity", the ratio of the radiation intensity in a given direction from the antenna to the radiation intensity averaged over all directions (Supporting Information). In this particular case, the directivity of SOA is approximately 50. This is an unexpected high value for an antenna only 2 μm in size.

In addition to the collection efficiency, the excitation rate of the QDs can also be improved by the SOA. It is known that dielectric microspheres can create a jet-like focus[42,43] and consequently enhance the excitation rate of the QDs. Different from the previously reported works, here, the SOA has an opaque magnetic core. To check whether it affects the focusing capability, simulation was performed, and the result shows that a narrow jet-like focus can still be formed despite the existence of an opaque core (Figure S3).

The above magnetic alignment technique is not limited to the perpendicular case. It can be applied to any desired positions by simply changing the direction of the magnetic fields. As shown in Figure 2, when the direction of magnetic fields, θ, was moved the position of SOA changed accordingly (Figure 2b). Meanwhile, the radiation pattern also changed dramatically, with the main radiation lobe moved from the center to the edge of the back focal plane (Figure 2c,d).

To understand the above phenomena, we simulated the radiation pattern of SOA at different positions with parameters used in the real experiment by sing FDTD method. When the lateral position of SOA moves from 0 to 0.6 μm, the main radiation lob is scanned from 0° to approximately 30° (Figure 2e,f). The results are consistent with the experimental observations (Figure 2c,d).

From the above results, it is evident that the radiation direction of the QD nanospot is sensitive to the position of SOA. Hereby, we plot the beam direction, θ_x, as the function of position of SOA, x (Figure 2g). The result shows that when the lateral position change is small the beam direction θ_x is linearly dependent on x with a slop of $d\theta_x/dx = 0.05°/nm$.

With the help of the $\theta_x - x$ curve, we can estimate the precision of the magnetic alignment method. Here, we take the normal alignment for example, the direction of the main radiation lobe is 1.9° from the normal (Figure 2c,d), corresponding to 38 nm lateral deviation from the QD spot. This is an exceptionally high

https://doi.org/10.1021/acs.nanolett.2c04981
Nano Lett. 2023, 23, 1539−1545

accuracy for a solution-phase self-assembly technique, which is intrinsically random.

To understand the extraordinary position control capability of the magnetic alignment method, a theorical model is studied, as shown in Figure 3. For simplicity, the SOAs and QD nanospots are treated as point magnetic dipole, $\mathbf{m}_{OA}$ and $\mathbf{m}_{QD}$, respectively. The interaction potential between them can then be explicated described as

$$V_{mag} = \frac{\mu_0}{4\pi}\frac{\mathbf{m}_{OA}\cdot\mathbf{m}_{QD} - 3(\mathbf{m}_{OA}\cdot\mathbf{e}_r)(\mathbf{m}_{QD}\cdot\mathbf{e}_r)}{r^3} \quad (1)$$

where $\mathbf{r} = |\mathbf{r}_{OA} - \mathbf{r}_{QD}|$, $\mathbf{r}_{OA}$, and $\mathbf{r}_{QD}$ is respectively the position of SOA and QDs, $\mathbf{e}_r$ is the unit vector along $\mathbf{r}$. In this work, B was in the range of 10−50 gauss. The induced magnetic dipole moments were calculated using the data reported by Yin's group (Section 5 in Supporting Information).[44] Assuming B = 30 gauss, we have $\mathbf{m}_{OA} = 4.90 \times 10^{-14}$ emu and $\mathbf{m}_{QD} = 6.38^{-18}$ emu. The potential distribution $V(r)$ with different magnetic field directions can then be calculated using eq 1. Here, we take the cases of $\theta = 0$ and 45° as examples, and the results are shown in Figure 3c,d.

It is evident that the magnetic interaction between SOAs and QD nanospots is a direction-dependent short-range interaction. The potential energy reaches its minimum when $\mathbf{m}_{OA}$ and $\mathbf{m}_{QD}$ are aligned along their local magnetic field line. The potential scales with $1/r^3$ and drops rapidly when r increases, dragging SOAs and QDs nanospots tightly close to each other. If we neglect the complexity caused by potential distribution, then the aligned position of SOA can then be estimated with a simple geometrical relation $x = R \cdot \tan\theta$. Here, R is the radius of the SOA and θ is the angle between B and the normal direction of the substrate (Figure 3a,b). This explains the field-dependent alignment position of SOAs in Figure 2.

In our experiment, the diameter of SOA was 2.2 μm SOA. Its center position was always at the z = 1.1 μm plane because of the dragging forces of the magnetic fields. We therefore plot the $V(x)$ curve at z = 1.1 μm, and a deep and narrow potential well can be observed (Figure 3e,f). The potential reaches −3.74 eV for a normal alignment ($\theta = 0°$) and −2.31 eV for $\theta = 45°$. They are 145 and 89 times higher than k_BT (0.026 eV), the kinetic energy of the random Brownian motion of the SOA, respectively. This will lead to strong and tight trapping of SOA at bottom of the potential well.

After knowing the trapping potential, we can further calculate the accuracy of this magnetic trapping of SOA with the help of Boltzmann distribution which describes the possibility distribution of occurrence at different positions of a particle, $P(\mathbf{r}) = \exp(-V(\mathbf{r})/k_BT)$. The results show a narrow position distribution of the SOA with a position uncertainly of ±40 nm and ±53 nm for $\theta = 0$ and 45°, respectively, as shown in Figure 3. They are consistent with the experimental observations in Figure 2.

Here, the position uncertainty can be further improved by increasing strength of magnetic fields. Considering that B was only 30 gauss in this work and this value can be increased by 1 order of magnitude with neodymium magnet, we can potentially push the position uncertainly down below 10 nm.

We also tested SOAs with different sizes and strong size-dependent behaviors were observed. In terms of magnetic alignment, smaller SOAs always lead to better performance since the magnetic interactions are strong enough to overcome other factors, namely, Brownian motions, gravity, and van der Waals forces. When the size of SOA increases, the magnetic interaction becomes weaker, the gravity, as well as van der Waals forces, becomes larger, and as the result, alignment becomes more difficult.

Moreover, the optical performance, particularly the directivity of SOAs is also size-dependent. As shown in Figure 4, when the

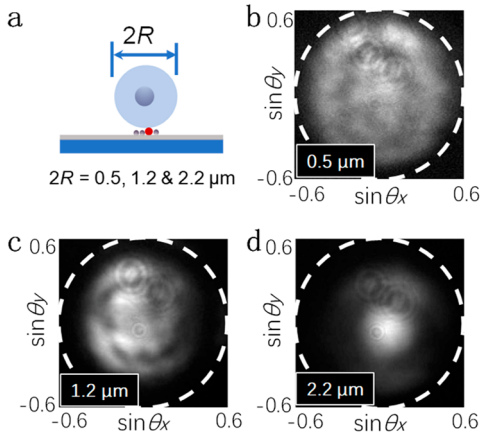

Figure 4. Size-dependent angular radiation of SOA. (a) Schematic drawing of the experiment. (b−d) Radiation pattern of SOA with different diameters (0.5, 1.2, and 2.2 μm).

diameter of the microsphere decreases from 2.2 to 0.6 μm, the width of main lobe increases from 16° to about 53°. This size-dependent radiation can be understood by thinking of the Heisenberg's uncertainty principle. It states that the product between the position uncertainly of photons (i.e., the size of the antenna) and the momentum uncertainty in the lateral direction (i.e., $k_0 \sin\theta$) is larger than 1/2. As a result, a smaller antenna will lead to a wider radiation lobe.

Finally, we would like to point out that the magnetic alignment technique of SOA is not limited to the above demonstrated QD clusters. It can be applied to various emitter systems, such as fluorescent molecules, upconversion nanocrystals and even a single quantum nanoemitter. With the help of the advanced nanoassembly techniques, emitters can be copatterned with magnetic NPs with nanometer precision, allowing us to further implement the magnetic alignment of SOAs.

In summary, we developed a new type of smart optical antennas which are chemically synthesized dielectric microsphere with a superparamagnetic core. These antennas can be precisely aligned on prepatterned magnetic QD nanospots in solution by simply applying external magnetic fields. After being aligned, the SOA can generate a beam-like emission as narrow as 16° and enhance the fluorescence signal by 11.8 times. Moreover, we demonstrated that the relative position between the antenna and QD nanospot, and consequently, the beam direction can be tuned with the magnetic fields. Theoretical analyses indicate that position accuracy of this magnetic alignment method can reach 40 nm. We believe that this smart optical antenna with its photon beaming capability and unique automatic alignment feature can have many important applications, particularly in the field of high efficiency bio/chem-sensors, as well as tunable nanophotonic devices.

https://doi.org/10.1021/acs.nanolett.2c04981
Nano Lett. 2023, 23, 1539−1545

METHODS

Synthesis of SOA. The superparamagnetic core (i.e., Fe_3O_4@SiO_2 core/shell colloids) of SOA was synthesized using the method reported by Yin's group.[45] First, an aqueous solution (3 mL) of Fe_3O_4 NPs was mixed with ethyl alcohol (20 mL) and ammonium hydroxide (28%, 1 mL) aqueous solution with vigorous stirring using mechanical stirrer. Then, TEOS (0.2 mL) was injected to the solution after ultrasonic stirring. After obtaining the desired size, the Fe_3O_4@SiO_2 colloids were collected by magnetic separation, washed with ethanol three times, and finally dispersed in ethanol (2 mL).

After obtaining superparamagnetic Fe_3O_4@SiO_2 cores, an additional polystyrene layer was coated to form optical antennas with seed emulsion polymerization. Fe_3O_4@SiO_2 colloids coupling with MPS were redispersed in ethanol (15 mL) with 130 mg of PVP and 1.67 mL of deionized water under sonication. After heated to 75 °C, a certain amount of AIBN/St was injected to the solution. The experiment was finished after 24 h.

Fabrication of Magnetic QD Nanospot Array. The magnetic QD nanospot arrays were fabricated by spinning mixture of Fe_3O_4 NP and QD solution (CdSe/ZnS core/shell NP, 660 nm emission, Suzhou Xingshuo Nanotech Co., Ltd.) on a prefabricated charge-patterned substrate using high-voltage AFM tip. Here, the bandgap of Fe_3O_4 NPs is larger than the photo energy of the fluorescence emission of the QDs. Therefore, they do not cause any signal loss.

Magnetic Alignment Technique. The experiments were performed in a 1 mm thick fluidic cell. To align the SOAs, a permanent magnetic was placed above the QDs nanospot array. SOAs were then dragged toward the QD nanospots to complete the alignment automatically (Figure S2). Here, the substrate was coated with a thin layer of fluoride polymer. Its low surface energy can prevent the unwanted absorption of the SOA by van der Waals forces effectively.

Simulation. Numerical simulations were performed using a commercial full 3D electromagnetic field solver (Lumerical FDTD) and the angular radiation patterns were calculated by using near-to-far field projection technique.

Optical Characterization. The performance of MOAs was measured with a home-built system, which can take images at the sample plane and the back focal plane (i.e., the Fourier plane) of the objective simultaneously. The excitation wavelength was 532 nm, and QDs emitted at 660 nm. The detailed setup can be found in Figure S1.

ASSOCIATED CONTENT

Supporting Information

The Supporting Information is available free of charge at https://pubs.acs.org/doi/10.1021/acs.nanolett.2c04981.

Optical characterization, magnetic alignment of a SOA, beamwidth, directivity, forward-to-backward ratio of SOA, focusing effect of SOA, magnetic dipole moment of superparamagnetic nanoparticles (PDF)

AUTHOR INFORMATION

Corresponding Authors

Yan-qing Lu − *College of Engineering and Applied Sciences, Jiangsu Key Laboratory of Artificial Functional Materials, MOE Key laboratory of Intelligent Optical Sensing and Manipulation, Nanjing University, Nanjing 210023, PR China;* orcid.org/0000-0001-6151-8557; Email: yqlu@nju.edu.cn

Zhenda Lu − *College of Engineering and Applied Sciences, Jiangsu Key Laboratory of Artificial Functional Materials, MOE Key laboratory of Intelligent Optical Sensing and Manipulation, Nanjing University, Nanjing 210023, PR China; State Key Laboratory of Analytical Chemistry for Life Science, Nanjing 210023, PR China;* orcid.org/0000-0002-9616-8814; Email: luzhenda@nju.edu.cn

Weihua Zhang − *College of Engineering and Applied Sciences, Jiangsu Key Laboratory of Artificial Functional Materials, MOE Key laboratory of Intelligent Optical Sensing and Manipulation, Nanjing University, Nanjing 210023, PR China; State Key Laboratory of Analytical Chemistry for Life Science, Nanjing 210023, PR China;* orcid.org/0000-0003-1743-5919; Email: zwh@nju.edu.cn

Authors

Luping Wang − *College of Engineering and Applied Sciences, Jiangsu Key Laboratory of Artificial Functional Materials, MOE Key laboratory of Intelligent Optical Sensing and Manipulation, Nanjing University, Nanjing 210023, PR China*

Zaiqin Man − *College of Engineering and Applied Sciences, Jiangsu Key Laboratory of Artificial Functional Materials, MOE Key laboratory of Intelligent Optical Sensing and Manipulation, Nanjing University, Nanjing 210023, PR China*

Yang Liu − *College of Engineering and Applied Sciences, Jiangsu Key Laboratory of Artificial Functional Materials, MOE Key laboratory of Intelligent Optical Sensing and Manipulation, Nanjing University, Nanjing 210023, PR China*

Ying Yu − *College of Engineering and Applied Sciences, Jiangsu Key Laboratory of Artificial Functional Materials, MOE Key laboratory of Intelligent Optical Sensing and Manipulation, Nanjing University, Nanjing 210023, PR China*

Chenyu Dong − *College of Engineering and Applied Sciences, Jiangsu Key Laboratory of Artificial Functional Materials, MOE Key laboratory of Intelligent Optical Sensing and Manipulation, Nanjing University, Nanjing 210023, PR China*

Jie Bian − *College of Engineering and Applied Sciences, Jiangsu Key Laboratory of Artificial Functional Materials, MOE Key laboratory of Intelligent Optical Sensing and Manipulation, Nanjing University, Nanjing 210023, PR China*

Complete contact information is available at: https://pubs.acs.org/10.1021/acs.nanolett.2c04981

Author Contributions

[§]L.W. and Z.M. contributed equally to this paper. The manuscript was written through contributions of all authors. All authors have given approval to the final version of the manuscript.

Funding

National Key Technologies R&D Program of China (No. 2021YFA1400803), National Natural Science Foundation of China (No. 22075128) and Natural Science Foundation of Jiangsu Province, Major Project (BK20212004).

Notes

The authors declare no competing financial interest.

REFERENCES

(1) Brutting, W.; Frischeisen, J.; Schmidt, T. D.; Scholz, B. J.; Mayr, C. Device efficiency of organic light-emitting diodes: Progress by improved light outcoupling. *Phys. Status Solidi A-Appl. Mater.* **2013**, *210*, 44−65.

(2) Song, J. J.; Wang, O.; Shen, H. B.; Lin, Q. L.; Li, Z. H.; Wang, L.; Zhang, X. T.; Li, L. S. Over 30% External Quantum Efficiency Light-Emitting Diodes by Engineering Quantum Dot-Assisted Energy Level Match for Hole Transport Layer. *Adv. Funct. Mater.* **2019**, *29*, 1808377.

(3) Michler, P.; Kiraz, A.; Becher, C.; Schoenfeld, W. V.; Petroff, P. M.; Zhang, L. D.; Hu, E.; Imamoglu, A. A quantum dot single-photon turnstile device. *Science* **2000**, *290*, 2282−2285.

(4) Lee, K. G.; Chen, X. W.; Eghlidi, H.; Kukura, P.; Lettow, R.; Renn, A.; Sandoghdar, V.; Gotzinger, S. A planar dielectric antenna for directional single-photon emission and near-unity collection efficiency. *Nat. Photonics* **2011**, *5*, 166−169.

(5) Yang, H.; Cornaglia, M.; Gijs, M. A. M. Photonic Nanojet Array for Fast Detection of Single Nanoparticles in a Flow. *Nano Lett.* **2015**, *15*, 1730−1735.

(6) Yang, H.; Gijs, M. A. M. Micro-optics for microfluidic analytical applications. *Chem. Soc. Rev.* **2018**, *47*, 1391−1458.

(7) Balanis, C. A. *Antenna Theory: Analysis and Design*. 3rd ed.; Wiley-Interscience: 2005; pp 27−108.

(8) Milligan, T. A. *Modern Antenna Design*. 2nd ed.; John Wiley & Sons, Inc.: 2005; pp 1−101.

(9) Hansen, R.; Collin, R. *Small Antenna Handbook*. John Wiley and Sons Ltd.: 2011; pp 1−58.

(10) Novotny, L.; van Hulst, N. Antennas for light. *Nat. Photonics* **2011**, *5*, 83−90.

(11) Biagioni, P.; Huang, J. S.; Hecht, B. Nanoantennas for visible and infrared radiation. *Rep. Prog. Phys.* **2012**, *75*, No. 024402.

(12) Curto, A. G.; Volpe, G.; Taminiau, T. H.; Kreuzer, M. P.; Quidant, R.; van Hulst, N. F. Unidirectional Emission of a Quantum Dot Coupled to a Nanoantenna. *Science* **2010**, *329*, 930−933.

(13) Jun, Y. C.; Huang, K. C. Y.; Brongersma, M. L. Plasmonic beaming and active control over fluorescent emission. *Nat. Commun.* **2011**, *2*, 283.

(14) Au, T. H.; Buil, S.; Quelin, X.; Hermier, J. P.; Lai, N. D. High Directional Radiation of Single Photon Emission in a Dielectric Antenna. *ACS Photonics* **2019**, *6*, 3024−3031.

(15) Kullock, R.; Ochs, M.; Grimm, P.; Emmerling, M.; Hecht, B. Electrically-driven Yagi-Uda antennas for light. *Nat. Commun.* **2020**, *11*, 115.

(16) Zhu, F. J.; Sanz-Paz, M.; Fernandez-Dominguez, A. I.; Zhuo, X. L.; Liz-Marzan, L. M.; Stefani, F. D.; Pilo-Pais, M.; Acuna, G. P. DNA-Templated Ultracompact Optical Antennas for Unidirectional Single-Molecule Emission. *Nano Lett.* **2022**, *22*, 6402−6408.

(17) Meng, Y.; Cheng, G.; Man, Z. Q.; Xu, Y.; Zhou, S.; Bian, J.; Lu, Z. D.; Zhang, W. H. Deterministic Assembly of Single Sub-20 nm Functional Nanoparticles Using a Thermally Modified Template with a Scanning Nanoprobe. *Adv. Mater.* **2020**, *32*, 2005979.

(18) Cheng, G.; Wang, Z.; Man, Z. Q.; Meng, Y.; Chen, M. L.; Bian, J.; Lu, Z. D.; Zhang, W. H. Single CdSe Quantum Dots Positioned in Nanostructured Heterogeneous Templates: Implications for High-Precision Nanoassembly. *ACS Appl. Nano Mater.* **2022**, *5*, 5756−5763.

(19) Farahani, J. N.; Pohl, D. W.; Eisler, H. J.; Hecht, B. Single quantum dot coupled to a scanning optical antenna: A tunable superemitter. *Phys. Rev. Lett.* **2005**, *95*, No. 017402.

(20) Anger, P.; Bharadwaj, P.; Novotny, L. Enhancement and quenching of single-molecule fluorescence. *Phys. Rev. Lett.* **2006**, *96*, 113002.

(21) Kuhn, S.; Hakanson, U.; Rogobete, L.; Sandoghdar, V. Enhancement of single-molecule fluorescence using a gold nanoparticle as an optical nanoantenna. *Phys. Rev. Lett.* **2006**, *97*, No. 017402.

(22) Pan, B. Y.; Yang, Y. L.; Bian, J.; Hu, X. P.; Zhang, W. H. Quantum dot decorated nano-pyramid fiber tip for scanning near-field optical microscopy. *Opt. Commun.* **2019**, *445*, 273−276.

(23) Lyu, Y. K.; Ji, Z. T.; He, T.; Lu, Z. D.; Zhang, W. H. Automated pick-and-place of single nanoparticle using electrically controlled low-surface energy nanotweezer. *AIP Adv.* **2021**, *11*, No. 035219.

(24) Mao, Y. F.; Pan, Y. N.; Zhang, W. H.; Zhu, R.; Xu, J.; Wu, W. G. Multi-Direction-Tunable Three-Dimensional Meta-Atoms for Reversible Switching between Midwave and Long-Wave Infrared Regimes. *Nano Lett.* **2016**, *16*, 7025−7029.

(25) Meng, C.; Thrane, P. C. V.; Ding, F.; Gjessing, J.; Thomaschewski, M.; Wu, C.; Dirdal, C.; Bozhevolnyi, S. I. Dynamic piezoelectric MEMS-based optical metasurfaces. *Sci. Adv.* **2021**, *7*, eabg5639.

(26) Earl, S. K.; James, T. D.; Davis, T. J.; McCallum, J. C.; Marvel, R. E.; Haglund, R. F.; Roberts, A. Tunable optical antennas enabled by the phase transition in vanadium dioxide. *Opt. Express* **2013**, *21*, 27503−27508.

(27) Wang, Y. F.; Landreman, P.; Schoen, D.; Okabe, K.; Marshall, A.; Celano, U.; Wong, H. S. P.; Park, J.; Brongersma, M. L. Electrical tuning of phase-change antennas and metasurfaces. *Nat. Nanotechnol.* **2021**, *16*, 667−672.

(28) Lu, Z. D.; Yin, Y. D. Colloidal nanoparticle clusters: functional materials by design. *Chem. Soc. Rev.* **2012**, *41*, 6874−6887.

(29) Talapin, D. V.; Shevchenko, E. V. Introduction: Nanoparticle Chemistry. *Chem. Rev.* **2016**, *116*, 10343−10345.

(30) Baek, W.; Chang, H.; Bootharaju, M. S.; Kim, J. H.; Park, S.; Hyeon, T. Recent Advances and Prospects in Colloidal Nanomaterials. *JACS Au* **2021**, *1*, 1849−1859.

(31) Yoshida, M.; Lahann, J. Smart nanomaterials. *ACS Nano* **2008**, *2*, 1101−1107.

(32) He, L.; Wang, M. S.; Ge, J. P.; Yin, Y. D. Magnetic Assembly Route to Colloidal Responsive Photonic Nanostructures. *Acc. Chem. Res.* **2012**, *45*, 1431−1440.

(33) Li, Z. W.; Yang, F.; Yin, Y. D. Smart Materials by Nanoscale Magnetic Assembly. *Adv. Funct. Mater.* **2020**, *30*, 1903467.

(34) Krasnok, A. E.; Miroshnichenko, A. E.; Belov, P. A.; Kivshar, Y. S. Huygens optical elements and Yagi-Uda nanoantennas based on dielectric nanoparticles. *Jetp Lett.* **2011**, *94*, 593−598.

(35) Krasnok, A. E.; Miroshnichenko, A. E.; Belov, P. A.; Kivshar, Y. S. All-dielectric optical nanoantennas. *Opt. Express* **2012**, *20*, 20599−20604.

(36) Chen, Z. G.; Taflove, A.; Backman, V. Photonic nanojet enhancement of backscattering of light by nanoparticles: a potential novel visible-light ultramicroscopy technique. *Opt. Express* **2004**, *12*, 1214−1220.

(37) Itagi, A. V.; Challener, W. A. Optics of photonic nanojets. *J. Opt. Soc. Am. A* **2005**, *22*, 2847−2858.

(38) Krasnok, A. E.; Simovski, C. R.; Belov, P. A.; Kivshar, Y. S. Superdirective dielectric nanoantennas. *Nanoscale* **2014**, *6*, 7354−7361.

(39) Sergeeva, K. A.; Tutov, M. V.; Voznesenskiy, S. S.; Shamich, N. I.; Mironenko, A. Y.; Sergeev, A. A. Highly-sensitive fluorescent detection of chemical compounds via photonic nanojet excitation. *Sens. Actuator B-Chem.* **2020**, *305*, 127354.

(40) Wenger, J.; Gerard, D.; Aouani, H.; Rigneault, H. Disposable microscope objective lenses for fluorescence correlation spectroscopy using latex microspheres. *Anal. Chem.* **2008**, *80*, 6800−6804.

(41) Xing, X.; Man, Z.; Bian, J.; Yin, Y.; Zhang, W.; Lu, Z. High-resolution combinatorial patterning of functional nanoparticles. *Nat. Commun.* **2020**, *11*, 6002.

(42) Gérard, D.; Wenger, J.; Devilez, A.; Gachet, D.; Stout, B.; Bonod, N.; Popov, E.; Rigneault, H. Strong electromagnetic confinement near dielectric microspheres to enhance single-molecule fluorescence. *Opt. Express* **2008**, *16*, 15297−15303.

(43) Yang, H.; Trouillon, R.; Huszka, G.; Gijs, M. A. Super-Resolution Imaging of a Dielectric Microsphere Is Governed by the Waist of Its Photonic Nanojet. *Nano Lett.* **2016**, *16*, 4862−70.

(44) Ge, J.; Hu, Y.; Biasini, M.; Beyermann, W. P.; Yin, Y. Superparamagnetic magnetite colloidal nanocrystal clusters. *Angew. Chem., Int. Ed.* **2007**, *46*, 4342−5.

https://doi.org/10.1021/acs.nanolett.2c04981
Nano Lett. 2023, 23, 1539−1545

(45) Ge, J.; Hu, Y.; Zhang, T.; Yin, Y. Superparamagnetic composite colloids with anisotropic structures. *J. Am. Chem. Soc.* **2007**, *129*, 8974−8975.

https://doi.org/10.1021/acs.nanolett.2c04981
Nano Lett. 2023, 23, 1539−1545